# Comparisons of dynamic triggering near Beijing, China following recent large earthquakes in Sumatra

Jing Wu,[1] Zhigang Peng,[2] Weijun Wang,[3] Xuan Gong,[3] Qifu Chen,[1] and Chunquan Wu[4]

Received 9 August 2012; revised 12 October 2012; accepted 15 October 2012; published 10 November 2012.

[1] Dynamic triggering around the Fangshan Pluton near Beijing is repeatedly identified. Here we report clear triggered events in this region during the surface waves of the 2012 Mw8.6 Sumatra earthquake. However, we do not find any triggered events during the G2 waves of the Mw8.6 event, and the surface waves of the Mw8.2 Sumatra earthquake that occurred two hours later. The peak ground velocities of the 2012 Mw8.2 event are around the apparent triggering threshold of 0.1–0.2 cm/s in this region. Hence, the fact that this event did not trigger does not require an influence of elapsed time since last trigger (the Mw8.6 mainshock), but is consistent with it. The lack of triggering during the G2 wave of the 2012 Mw8.6 mainshock may be caused by relatively weak surface-wave signals in the intermediate period of 100–10 s. **Citation:** Wu, J., Z. Peng, W. Wang, X. Gong, Q. Chen, and C. Wu (2012), Comparisons of dynamic triggering near Beijing, China following recent large earthquakes in Sumatra, *Geophys. Res. Lett.*, *39*, L21310, doi:10.1029/2012GL053515.

## 1. Introduction

[2] Dynamically triggered earthquakes have been widely observed at different tectonic environments. These include active plate boundary faults, geothermal/volcanic regions with active background seismicity [*Hill and Prejean*, 2007, and references therein], and intraplate regions with low background seismicity [e.g., *Jiang et al.*, 2010; *Gonzalez-Huizar and Velasco*, 2011]. Compared with static and quasi-static triggering that only occur within a few rupture lengths of a mainshock, dynamic triggering could reach to thousands of kilometers away and is mostly caused by transient stresses associated with large amplitude surface waves. The main factors affecting the triggering potential include the peak ground velocity (PGV), frequency content and the incident angle of the triggering wave [*Wu et al.*, 2011], background seismicity and ambient conditions around the triggered sites [*Gomberg*, 2010].

[3] Recently, *Daniel et al.* [2008] compared the triggering behavior of two Ms6.6 earthquakes occurred in southern Iceland in 2000 that were separated by 3 days. They found that the second mainshock triggered a much smaller percentage of earthquakes as compared with the first one, despite their similar magnitudes. They suggested that the first mainshock may have depleted the nucleation points available for rupture, and it took time for them to become available. Based on the high seismicity rate and lack of widespread triggering in Japan, *Harrington and Brodsky* [2006] proposed another model where frequent occurrence of shaking may prevent the formation of clogged fractures available for triggering effects via fracture unclogging [*Brodsky et al.*, 2003]. These recent studies suggest that time since previous trigger could be another factor that control the triggering behavior. However, it is not clear whether other factors also contribute and which plays the most important role in controlling the triggering behavior.

[4] In this study, we focus on dynamic triggering around the Fangshan region near Beijing, China (Figure 1), which is located at the border between the Taihang mountain and the North China basin. The Fangshan Pluton was formed during a dioritic intrusion at c. 130 Ma. Its lithological boundary to the host rock is characterized by aureole-shape ductile shear zones. Dynamically triggered earthquakes have been repeatedly observed around this region [*Peng et al.*, 2010; *Jiang et al.*, 2010; *Wu et al.*, 2011; *Wang et al.*, 2011]. The triggered events are shown as clear P and S waves in the 5 Hz high-pass-filtered three-component seismograms during the passing surface waves of large distant earthquakes.

[5] Here we examine dynamic triggering around the Fangshan region following the most recent 2012/04/11 Mw8.6 Sumatra earthquake and its large Mw8.2 aftershock that occurred 2 hours later. These two earthquakes have caused a transient increase of global seismicity, mainly due to their large-amplitude Love waves excited by the strike-slip faultings [*Pollitz et al.*, 2012]. In addition, the relative short duration between the two Mw $\geq$ 8 events allow us to examine the recurrence time of dynamic triggering since last trigger [e.g., *Daniel et al.*, 2008] and other factors (e.g., PGVs, frequency content) that control triggering around Fangshan pluton.

## 2. Data and Analysis Procedure

[6] The seismic data analyzed in this study is recorded by the Beijing digital seismic network BJ (operated by the Beijing Earthquake Administration) and BU (operated by Institute of Geophysics, China Earthquake Administration). There are 49 stations in the BJ and BU networks, of which 35 have broadband sensors, and 14 have short-period sensors. Following our previous studies [*Peng et al.*, 2010; *Wu et al.*, 2011], we download the continuous waveforms 8 hours before and after the first 2012 Sumatra earthquake from both networks. We also include the waveforms recorded by the broadband station BJT that belongs to the New

[1]Institute of Geology and Geophysics, Chinese Academy of Sciences, Beijing, China.
[2]School of Earth and Atmospheric Sciences, Georgia Institute of Technology, Atlanta, Georgia, USA.
[3]Institute of Earthquake Science, China Earthquake Administration, Beijing, China.
[4]Geophysics Group, Los Alamos National Laboratory, Los Alamos, New Mexico, USA.

Corresponding author: J. Wu, Institute of Geology and Geophysics, Chinese Academy of Sciences, 19 West Beitucheng, Chaoyang District, Beijing 100029, China. (xianhua123@yahoo.com)

This paper is not subject to U.S. copyright.
Published in 2012 by the American Geophysical Union.

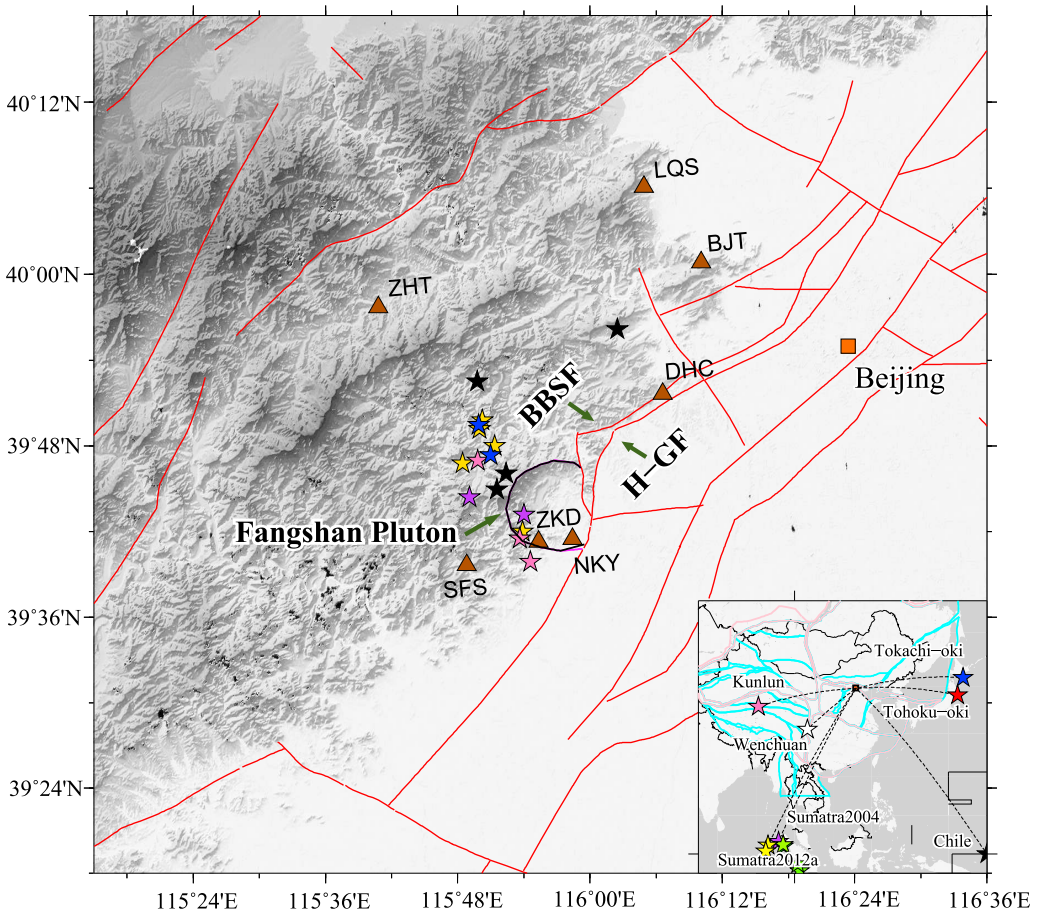


**Figure 1.** Map view of the study region around Beijing, China. Triangles mark seismic stations from the BJ, BU, and IC networks. Red lines show major faults in the study area, with the Babaoshan Fault (BBSF), and Huangzhuang Gaoliying Fault (H-GF) marked. The stars show locations of local earthquakes triggered by several teleseismic earthquakes, and the colors of the triggered earthquakes correspond to those of the triggering mainshock shown in the inset. The inset shows a map around China with the box corresponds to the study region.

China Digital Seismic Network (IC). In addition, we re-examine the waveforms for other 5 Sumatra earthquakes (2004 Mw9.2, 2005 Mw8.6, 2007 Mw8.5, 2007 Mw7.9 and 2010 Mw7.8) and use them for comparison.

[7] The analysis procedure generally follows that of *Wu et al.* [2011] and is briefly described here. First, we apply a 5 Hz high-pass filter on three components of all possible stations around the Fangshan Pluton. Next, we visually inspect the filtered trace together with the instrument-corrected broadband seismograms to identify possible triggered signals during the large-amplitude surface waves of the two Sumatra earthquakes. To evaluate the statistical significance of triggered earthquakes, we sum the number of points in the stacked high-pass-filtered function [*Jiang et al.*, 2010] at stations NKY and BJT that are above certain threshold during the teleseismic surface waves (with apparent velocity of 5–2 km/s) and the 8-hour period before the mainshock respectively, and then compute the ß–statistic value [*Aron and Hardebeck*, 2009]. Here we use 6, 9 and 12 times the median absolute deviation (MAD) of the envelope 8 hours before the mainshock (Table S1 in the auxiliary material).[1] We consider the triggering as statistically significant if the ß–values for 2 out of 3 MAD values are larger than 2.

[8] We then hand-pick the P and S arrivals at all possible stations for each earthquake, and use the Hypo71 program to locate the event. We also measure the local magnitude *M*L of each event according to the peak amplitude averaged over two horizontal components and the *S-P* times [*Peng et al.*, 2010].

## 3. General Observations

[9] Figure 2 shows a comparison of high-pass-filtered envelope functions at stations BJT and NKY and the broadband displacement seismograms at station NKY. While some high-frequency signals occurred before and after both mainshocks, the amplitudes during the surface waves of the first Mw8.6 Sumatra mainshock are much larger than those at other times. The corresponding ß–values for different thresholds are also larger than 2 (Table S1), suggesting that the triggering is statistically significant. In comparison, the ß–values for the G2 waves (i.e., Love waves circling around the other side of the earth) and the direct surface waves for the Mw8.2 Sumatra earthquake that occurred 2 hours later are less than 2, indicating a lack of clear triggering during these time windows.

[1]Auxiliary materials are available in the HTML. doi:10.1029/2012GL053515.

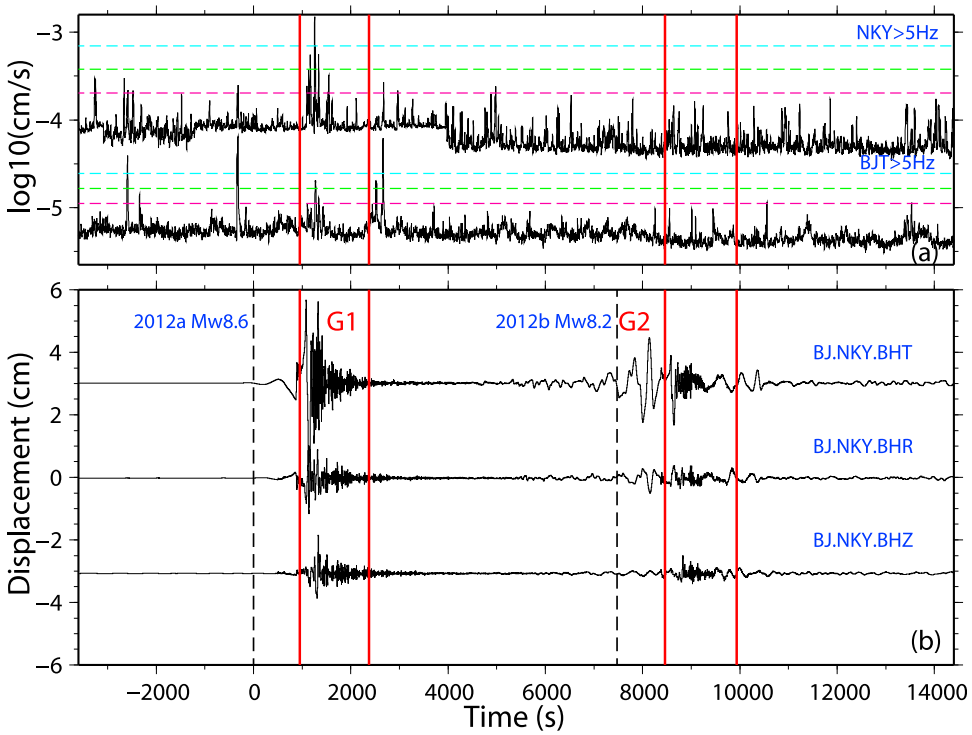


**Figure 2.** (a) Stacked 5-Hz high-pass filtered envelope functions at station NKY and BJT showing both background activities and triggered earthquakes during the 2012 Mw8.6 and Mw8.2 Sumatra earthquakes. The two red lines mark the time window of large-amplitude surface waves corresponding to the apparent velocity of 5 and 2 km/s. The red, green and cyan dashed lines mark the 6, 9 and 12 times the median absolute deviation (MAD) values calculated from the envelope before the mainshock. The envelope at station BJT is shifted downward by 0.8 for plotting purpose. (b) Three-component displacement seismograms recorded at station NKY showing the teleseismic waves of the two 2012 Sumatra earthquakes, and the G2 waves of the Mw8.6 mainshock

[10] A zoom-in plot (Figure 3) during the direct surface waves of the first Mw8.6 mainshock shows further evidence of dynamically triggered earthquakes around the study region. Coherent high-frequency signals with double peaks were recorded at stations ZKD, NKY and SFS around the Fangshan Pluton. Stations ZHT, BJT and LQS also recorded triggered signals although they are not as clear as the previous three stations. The microearthquakes were triggered during the first cycle of the Love wave, and became further intensified during the subsequent Love and Rayleigh waves. These triggered events are located at shallow depth (<5 km) near the Fangshan Pluton (Figure 1), and their magnitudes are in the range of 1–2, consistent with those from the previous studies [*Wu et al.*, 2011; *Wang et al.*, 2011].

[11] Figure S1 shows a similar plot for the Mw8.2 Sumatra aftershock. Stations NKY and ZKD with clear triggered events during the first mainshock did not record any coherent high-frequency signals during the surface waves of the Mw8.2 event. Station SFS recorded several high-frequency signals, but no clear double peaks could be identified and they were not coherent at nearby stations. We also do not observe any clear triggered signals during the long-period G2 wave of the first mainshock, which arrived around the teleseismic P wave of the Mw8.2 Sumatra earthquake.

## 4. Other Recent Sumatra Earthquakes

[12] In order to better understand why the Mw8.2 2012 Sumatra earthquake did not trigger local events around the Fangshan region, we follow the same procedure as before and re-examine the seismic records for another 5 earthquakes occurred around Sumatra since 2004. These include the 2004 Mw9.2 Sumatra, the 2005 Mw8.6 Nias, the 2007 Mw8.5, 2007 Mw7.9 and the 2010 Mw7.8 Sumatra earthquakes. *Wu et al.* [2011] analyzed the first three events and found that only the 2004 Sumatra earthquake has triggered earthquakes in our study region. Figure S2 also show clear high-frequency signals during the passage of S, Love and Rayleigh waves of the 2004 Sumatra earthquake, and the ß–statistic values are well above 2 for 3 MAD values. We determine the locations and magnitudes of two triggered events with larger amplitudes, and the obtained results are close to those found in this and previous studies [*Wu et al.*, 2011]. For the 2005 Nias earthquake, we are able to identify some earthquake-like signals during the surface waves at station NKY, but not at other stations, such as BJT (Figure S3). The corresponding ß-values show statistically significant triggering from the envelope function at NKY but not at BJT. Hence, we consider this case as not clear.

[13] Although the 2007 Mw8.5 has PGVs between 0.1–0.2 cm/s, we do not observe clearly triggered earthquakes (Figure S4). At NKY, the median background noise for this event is larger than those from other events (Figure 4a), which could possibly cover potential triggered earthquakes. In addition, waveforms at SFS, DHC, ZHT, BJT and LQS are noisy, and station ZKD has no data, thus these stations could not be used further. Hence, we also consider this event as not clear. Finally, we do not observe any triggered earthquakes for the 2007 Mw7.9 and the 2010 Mw7.8

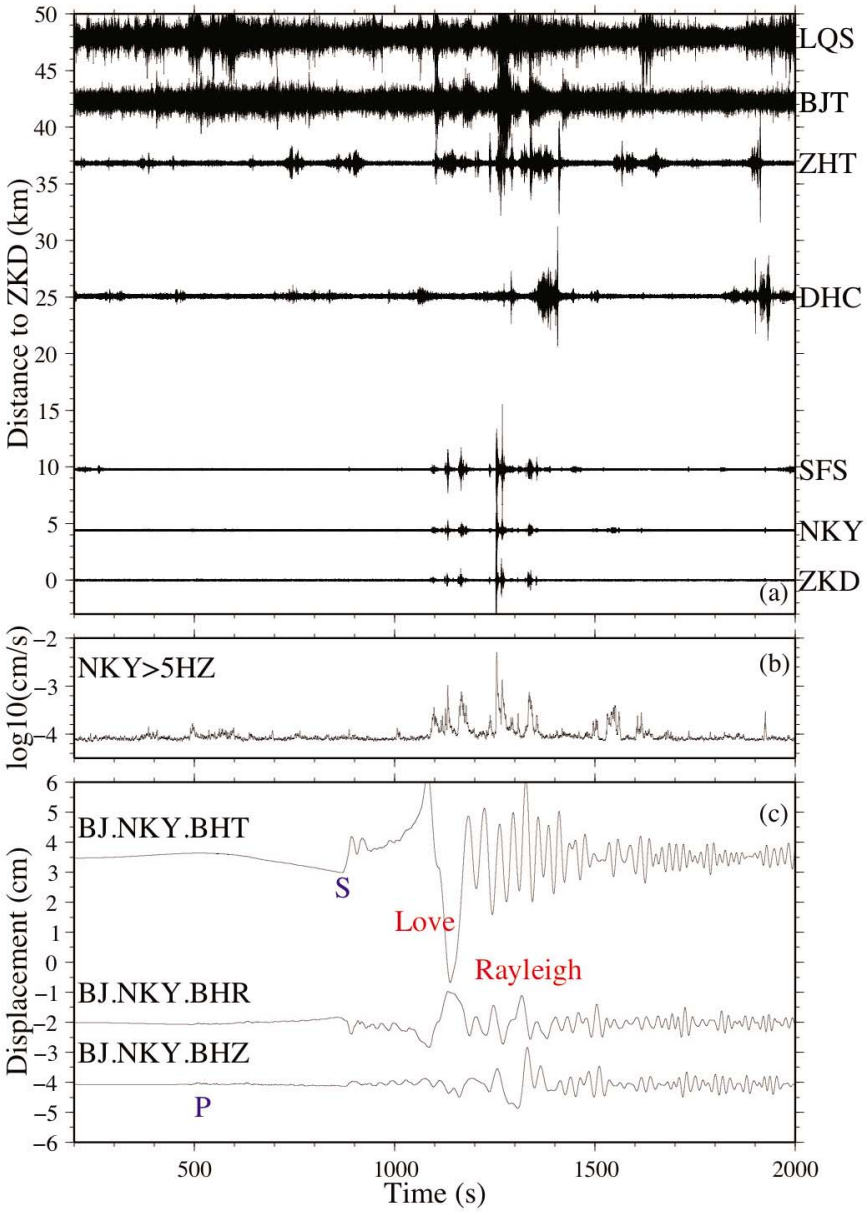


**Figure 3.** (a) 5-Hz high-pass filtered seismograms aligned by the distance to station ZKD showing triggered microearthquakes during the surface waves of the 2012 Mw8.6 Sumatra earthquake. (b) Stacked 5-Hz high-pass filtered envelope function at station NKY. (c) Three-component displacement waveforms at station NKY showing the teleseismic waves of the Mw8.6 mainshock.

Sumatra earthquakes. Their ß–statistic values are less than 2, and their PGVs are less than 0.1 cm/s (Figures S5 and S6).

## 5. Relationship Between Dynamic Stresses and Triggered Earthquakes

[14] To better understand the relationship between dynamic stresses and triggered earthquakes, we compare the PGVs of the teleseismic waves with the peak high-frequency signals during the teleseismic waves. The main procedure generally follows that of *Chao et al.* [2012]. However, we measure the peak but not median values, mainly because earthquakes have impulsive signals with short duration, so the median high-frequency signals could be almost the same as the median background noise levels before the mainshock (~600 s before the P wave). We focus on the measurements at station NKY because it is close to the triggered earthquakes. Since we could not obtain the continuous waveforms at the station for all Mw ≥ 7.5 events since 2000, we only measure the PGVs and the peak high-frequency signals for the 12 events that we have waveforms at hand. As shown in Figure 4a, the peak high-frequency signals during the teleseismic surface waves of the 7 triggering mainshocks do not show a positive correlation with the transverse PGVs. If we include the measurements from the other 6 non-triggering/clear events, we do find a weak correlation with a correlation coefficient (CC) value of 0.61. We do not find any positive correlation between the peak high-frequency signals and the vertical PGVs (Figure S7). We also

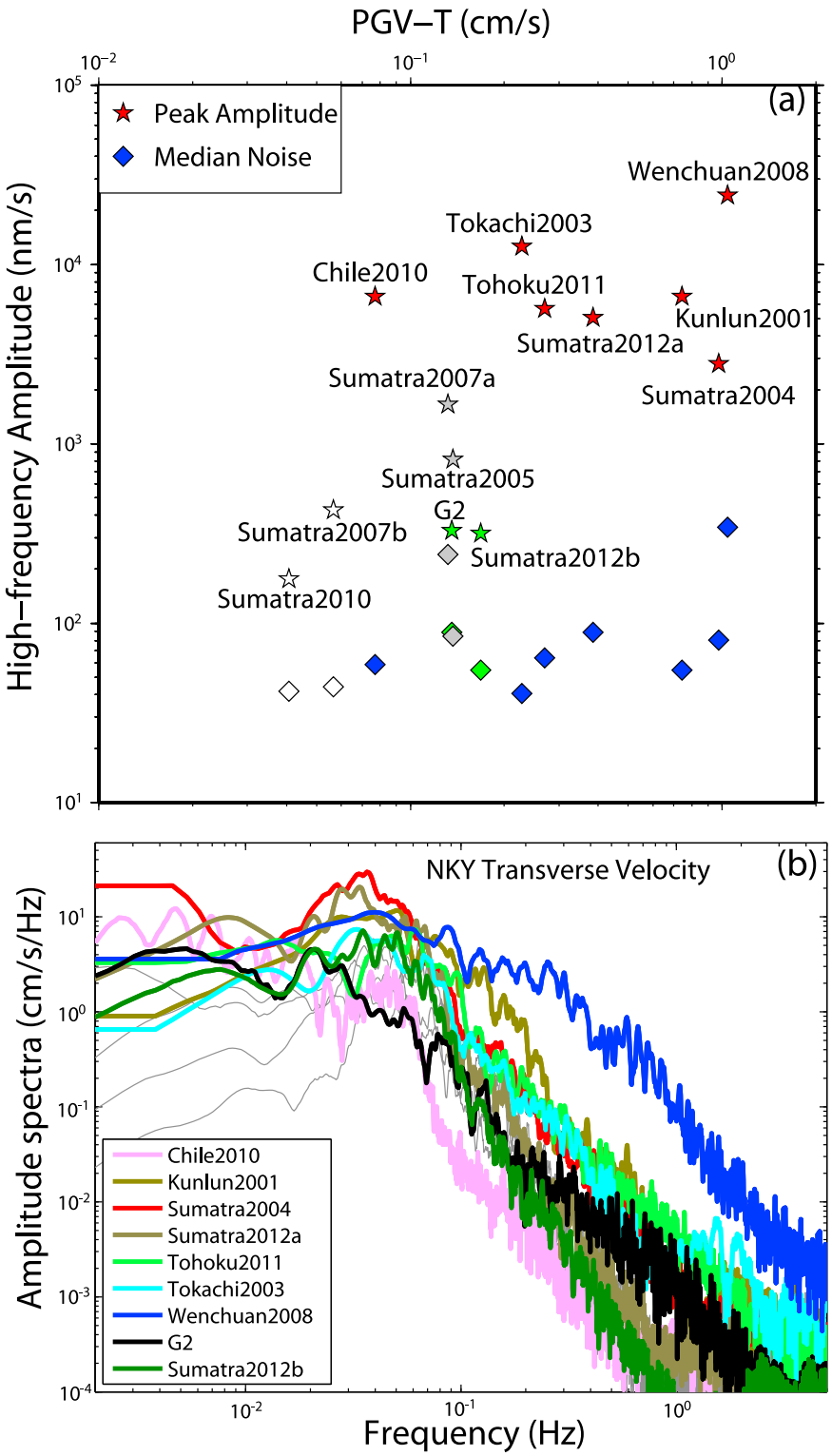


**Figure 4.** (a) Median high-frequency amplitudes before the mainshocks and peak high-frequency amplitudes during the teleseismic waves versus the corresponding peak ground velocity of transverse component (PGV-T) for all mainshocks at station NKY. The red, gray and open stars mark the events with triggered earthquakes, with not clear evidence, and without triggered earthquakes, respectively. The green stars mark the values for the 2012 Mw8.2 aftershock and the G2 of the 2012 Mw8.6 mainshock. (b) Comparison of the velocity spectra of the transverse component for the events used in Figure 4a. Thick colored lines show triggering events, and the gray lines show non-triggering and not-clear events. The spectra from the G2 of the Mw8.6 mainshock and the 2012 Mw8.2 aftershock are marked by thick black and green colors, respectively.

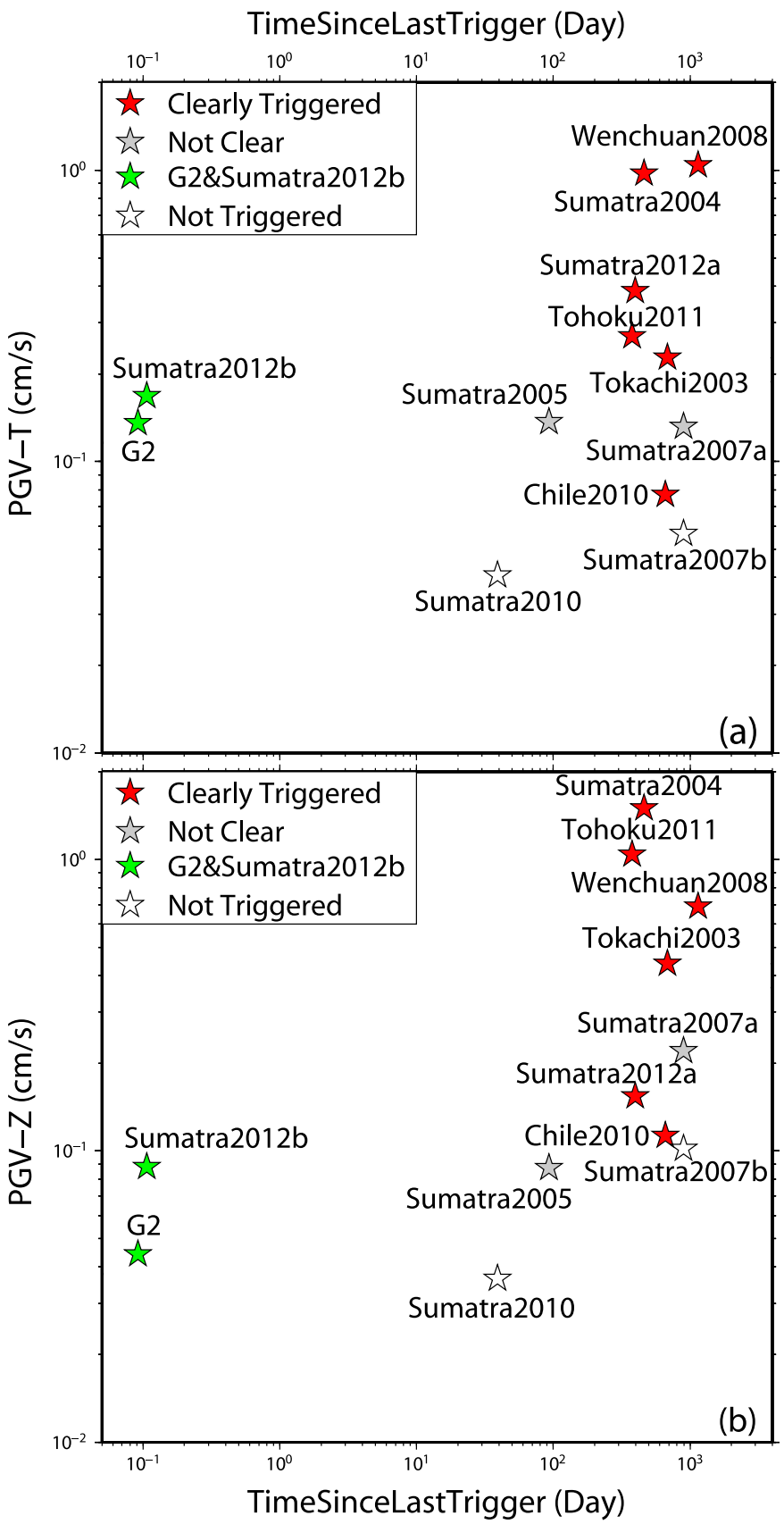


**Figure 5.** Peak ground velocities (PGVs) at station NKY versus the time since the last triggering event. Results on the (a) transverse and (b) vertical components. Red, grey, green and open stars mark events that correspond to clearly triggering, not clear, G2 wave of the 2012 Mw8.6 and 2012 Mw8.2, and not triggering, respectively.

measure the same parameters for all Mw ≥ 7.5 shallow events (distance > 1000 km, depth < 100 km) since 2000 at station IC. BJT (Figure S8). Similarly, the correlation between the PGVs and peak high-frequency amplitudes is not clear.

## 6. Frequency Content of the Triggering Waves

[15] We also quantify the frequency dependence of the triggering wave by examining the velocity spectra of all events analyzed in Figure 4a, following the method of *Peng et al.* [2009]. Figure 4b shows that for periods larger than 100 s, the spectra of the Mw8.2 Sumatra aftershock and G2 of the Mw8.6 Sumatra mainshock are in the middle range of the other spectra. The 2001 Kunlun and the 2003 Tokachi-Oki events have the lowest spectra values, although they triggered clear microearthquakes in our study region [*Wu et al.*, 2011]. In the periods of 100 to 10 s, the 2010 Mw8.8 Chile and the G2 of the 2012 Mw8.6 Sumatra events have the lowest spectra values, likely caused by attenuation after long propagation distance. The Mw8.2 Sumatra aftershock has similar spectrum shape with that of the 2003 Tokachi-Oki events in the transverse component (Figure 4b). However, the Tokachi-Oki event has higher spectral values than the Sumatra aftershock in the vertical component (Figure S9).

## 7. Elapsed Time Since Last Trigger

[16] Finally, we check whether the elapsed time since previously triggering event plays any role in controlling the triggering behavior. To examine this further, we plot the PGVs observed at station NKY versus the elapsed time since the previous event that have triggered in our study region (Figure 5). Obviously, the G2 of 2012 Mw8.6 and 2012 Mw8.2 Sumatra mainshocks have the shortest time of ~2 hours since the last trigger, which is the Mw8.6 mainshock. Except the 2005 Nias and 2010 Sumatra earthquakes, the other mainshocks occurred between 100–1000 days since last triggering events.

## 8. Discussion

[17] In this study we conducted a systematic study of dynamically triggered microearthquakes around the Fangshan Pluton SW of Beijing following the 2012 Mw8.6 and Mw8.2 Sumatra earthquakes. While the direct surface waves of the first Mw8.6 mainshock triggered clear earthquakes, we found no clear evidence of triggering during the subsequent G2 wave and the direct surface waves of the second Mw8.2 aftershock. The PGVs of the G2 wave for the Mw8.6 mainshock and the direct surface waves of the second Mw8.2 aftershock are close to the apparent triggering threshold of 0.1–0.2 cm/s as defined by other recent events (Figure 4a). Hence, a simple explanation is that their PGVs are not high enough to trigger activity in our study region. Unfortunately, we were unable to make a definitive conclusion for the effect of PGV on triggering behavior, mainly due to the lack of clear evidence for the 2005 Mw8.6 Nias and the 2007 Mw8.5 Sumatra earthquakes (Figure 4a). However, we did observe that the 2010 Mw8.8 Chile and the 2003 Mw8.3 Tokachi-Oki earthquakes have triggered microearthquakes in this region [*Wu et al.*, 2011; *Wang et al.*, 2011]. Both of them have their PGVs slightly smaller and larger than those of the G2 wave of the Mw8.6 and the direct surface wave of the Mw8.2 aftershock, respectively. These observations lead us to consider factors other than the PGVs that may affect the triggering behaviors.

[18] As shown in Figure 4b, while the G2 wave of the first Mw8.6 mainshock excited clear long-period signals (>100 s), it had a relatively low spectrum value in the intermediate period of 100–10 s. Hence, the lack of triggered earthquakes during the G2 wave could be related to the low-amplitude spectrum in this period range. This is also consistent with the conclusion that ultra-long-period signals (>100 s) are not critical for triggering tremor in Parkfield [*Peng et al.*, 2009] and Taiwan [*Chao et al.*, 2012]. The 2012 Mw8.2 Sumatra aftershock and the 2003 Mw8.3 Tokachi-Oki earthquake have similar spectra in the period range of 100–10 s (Figure 4b), yet the elapsed time since last trigger differ by several orders of magnitudes (Figure 5). Hence, while our observation does not require a role of the elapsed time since last trigger, it is at least consistent with it. Similarly, the PGV of the 2007 Mw7.9 Sumatra earthquake is close to the 2010 Chile event. Yet it did not trigger any seismicity. We suspect that it could be related to the fact it occurred only within 12 hours of the Mw8.5 Sumatra earthquake. However, we were unable to conclude whether this Mw8.5 event triggered in our study region or not, due to the lack of high quality data during that time period. Hence, whether the elapsed time played a role here or not remains open.

[19] We have attempted to quantify the triggering threshold with incidence angles and different fault types in our previous study [*Wu et al.*, 2011]. However, because the receiver fault geometry is not well known, their results did not provide any additional constraints on the triggering threshold/process. In addition, the locations of the triggered earthquakes were not well constrained with only three stations (NKY, ZKD and SFS) immediately around the Fangshan Pluton. Our next step is to analyze the seismic data during the 2011 Mw9.1 Tohoku-Oki earthquake recorded by a 11-station temporary network around the Fangshan Pluton [*Wang et al.*, 2011]. By accurately determining the hypocentral locations and the focal mechanisms of the triggered and background events, we hope to better understand the source faults and necessary conditions for dynamic triggering in this region.

[20] **Acknowledgments.** The seismic data analyzed in this study is obtained from the Data Management Centre of China National Seismic Network at Institute of Geophysics, China Earthquake Administration. We thank Kevin Chao and Zhongjie Zhang for their useful comments. This work was supported by the National Science Foundation EAR-0956051 (ZP) and National Science Foundation of China grants 41228005 (ZP, WW) and 41074037 and 41021063 (JW).

[21] The Editor thanks Stephanie Prejean and an anonymous reviewer for their assistance in evaluating this paper.

## References

Aron, A., and J. L. Hardebeck (2009), Seismicity rate changes along the central California coast due to stress changes from the 2003 M 6.5 San Simeon and 2004 M 6.0 Parkfield earthquakes, *Bull. Seismol. Soc. Am.*, *99*, 2280–2292, doi:10.1785/0120080239.

Brodsky, E. E., E. Roeloffs, D. Woodcock, I. Gall, and M. Manga (2003), A mechanism for sustained groundwater pressure changes induced by distant earthquakes, *J. Geophys. Res.*, *108*(B8), 2390, doi:10.1029/2002JB002321.

Chao, K., Z. Peng, C. Wu, C.-C. Tang, and C.-L. Lin (2012), Remote triggering of non-volcanic tremor around Taiwan, *Geophys. J. Int.*, *188*, 301–324, doi:10.1111/j.1365-246X.2011.05261.x.

Daniel, G., D. Marsan, and M. Bouchon (2008), Earthquake triggering in southern Iceland following the June 2000 Ms 6.6 doublet, *J. Geophys. Res.*, *113*, B05310, doi:10.1029/2007JB005107.

Gomberg, J. (2010), Lessons from (triggered) tremor, *J. Geophys. Res.*, *115*, B10302, doi:10.1029/2009JB007011.

Gonzalez-Huizar, H., and A. A. Velasco (2011), Dynamic triggering: Stress modeling and a case study, *J. Geophys. Res.*, *116*, B02304, doi:10.1029/2009JB007000.

Harrington, R. M., and E. E. Brodsky (2006), The absence of remotely triggered seismicity in Japan, *Bull. Seismol. Soc. Am.*, *96*, 871–878, doi:10.1785/0120050076.

Hill, D. P., and S. G. Prejean (2007), Dynamic triggering, in *Treatise on Geophysics*, vol. 4, *Earthquake Seismology*, edited by H. Kanamori, pp. 257–291, Elsevier, Amsterdam, doi:10.1016/B978-044452748-6.00070-5.

Jiang, T., Z. Peng, W. Wang, and Q. Chen (2010), Remotely triggered seismicity in continental China by the 2008 Mw 7.9 Wenchuan earthquake, *Bull. Seismol. Soc. Am.*, *100*(5B), 2574–2589, doi:10.1785/0120090286.

Peng, Z., J. E. Vidale, A. G. Wech, R. M. Nadeau, and K. C. Creager (2009), Remote triggering of tremor along the San Andreas Fault in central California, *J. Geophys. Res.*, *114*, B00A06, doi:10.1029/2008JB006049.

Peng, Z., W. Wang, Q. Chen, and T. Jiang (2010), Remotely triggered seismicity in north China following the 2008 Mw 7.9 Wenchuan earthquake, *Earth Planets Space*, *62*, 893–898, doi:10.5047/eps.2009.03.006.

Pollitz, F. F., R. S. Stein, and R. Burgmann (2012), The 11 April 2012 M = 8.6 East Indian Ocean earthquake triggered large aftershocks worldwide, *Nature*, *490*, 250–253, doi:10.1038/nature11504.

Wang, W., X. Gong, Z. Peng, Q. Chen, and C. Wu (2011), Dynamic triggering around Fangshan Pluton near Beijing, China, Abstract S22B-06 presented at 2011 Fall Meeting, AGU, San Francisco, Calif., 5–9 Dec.

Wu, C., Z. Peng, W. Wang, and Q. Chen (2011), Dynamic triggering of shallow earthquakes near Beijing, China, *Geophys. J. Int.*, *185*, 1321–1334, doi:10.1111/j.1365-246X.2011.05002.x.